Proceedings World Geothermal Congress 2026
Calgary, Canada, June 8 – 11, 2026

Review of Rock Testing in Brittle-Ductile Transition Conditions and Implications on Wellbore Stability in Ultra-Deep Drilling

Angel Sanchez-Barra*, Anna Rogers and Juan Arias
Eavor Technologies Inc.
angel.sanchez.barra@eavor.com

Keywords: Brittle–ductile transition; Borehole convergence; Brittle creep; Ultra-deep drilling

ABSTRACT

As global energy consumption continues to rise, the development of scalable and sustainable energy solutions is imperative to ensure that total energy supply can meet future demands. Ultra-deep geothermal energy offers a promising alternative by enabling localized, autonomous power generation at nearly any location on Earth. However, unlocking this potential requires drilling into ultra-deep conditions, where elevated temperatures and in situ stresses induce complex geomechanical behavior. In these ultra-deep conditions, rock deformation transition from brittle fracturing to semi-brittle and ultimately ductile flow, challenging conventional approaches to drilling and wellbore stability predictions. This study investigates the evolution of deformation mechanisms across the brittle-ductile transition (BDT) using a comprehensive review of literature data and previous experiences spanning microstructural observations, core-scale laboratory experiments, and field-scale measurements, including insights from the IDDP-2 geothermal project in Iceland, the KTB exploration borehole in Germany, Gravberg-1 in Sweden, and other relevant cases. Particular emphasis is placed on identifying how failure modes change with increasing stress-temperature conditions, the role of time-dependent creep in semi-brittle regimes, and the implications of these processes for borehole convergence and stress redistribution. By synthesizing data across scales and conditions, this work identifies future areas of research that will better inform geomechanical models and enable ultra-deep geothermal development.

1 INTRODUCTION

The development of ultra-deep geothermal systems demands significant technological advancements to overcome the challenges of drilling into hard basement rocks under high-pressure, high-temperature (HPHT) conditions. Unlike conventional geothermal systems, which typically operate in sedimentary formations or shallow crystalline units, ultra-deep systems target basement rocks at depths where temperatures exceed 300–400 °C and in situ stresses can reach several hundred MPa. Under such conditions, the rock may approach or intersect the brittle-ductile transition, a critical regime where deformation mechanisms shift from localized brittle fracture and frictional sliding to semi-brittle flow and eventually distributed ductile creep.

Rock behavior is governed by a complex interaction of in-situ stress, temperature, geological strain rates, mineral composition, and water saturation. These factors together control whether deformation is dominated by shear and tensile failure or by creep mechanisms such as dislocation motion, diffusion, and dissolution–precipitation. At the wellbore scale, this means that failure may occur not only through sudden tensile cracks and breakouts but also through time-dependent deformation, which can progressively alter wellbore geometry and compromise integrity during drilling and long-term operations. The semi-brittle domain, where both mechanisms operate simultaneously, is especially complex and remains a critical focus of experimental rock mechanics research. These processes are not merely theoretical, they have been observed repeatedly in deep drilling campaigns worldwide, most notably in the German Continental Deep Drilling Program (KTB) and the Siljan Ring borehole (Gravberg-1) in Sweden, where time-dependent deformation and stress redistribution were major limiting factors for drilling depth and stability (Borm et al., 1997; Stephansson et al., 1989).

This study reviews the current state of knowledge on deformation mechanisms across the brittle-ductile transition in basement rocks, with an emphasis on granite rock as a reference material. By integrating experimental data with field observations from ultra-deep boreholes, this study evaluates how temperature, confining stress, strain rate, and water saturation influence creep behavior and stability under HPHT conditions.

2 DEFORMATION MECHANISMS ACROSS THE BRITTLE–DUCTILE TRANSITION

The brittle–ductile transition represents a key regime in rock mechanics where deformation shifts from stress-dependent, fracture-dominated brittle behavior to temperature- and time-dependent ductile flow. Within this

transition lies a semi-brittle domain where both mechanisms act concurrently. Understanding the range of deformation mechanisms that operate in this transitional zone is critical for interpreting geomechanical responses and optimizing drilling in ultra-deep geothermal environments.

Brittle deformation, which is characteristic of breakouts and tensile failure, involves the nucleation and propagation of cracks through the breaking of atomic bonds and the creation of new surfaces, ultimately leading to frictional sliding. This process is typically accompanied by dilatancy as new fractures open and rock fragments slide past one another, performing work against the confining stress (Reber & Pec, 2018).

Semi-brittle deformation arises when both brittle and time-dependent mechanisms contribute significantly and concurrently to strain. Microstructurally, this regime reflects combined sensitivity to strain rate, temperature, and stress, displaying both dilatancy and defect mobility. Brittle and time-dependent processes may act sequentially or simultaneously. For instance, in serial semi-brittle deformation, fracture-induced grain-size reduction facilitates subsequent temperature-activated creep mechanisms due to their relatively low activation energy in gouge zones. In contrast, parallel semi-brittle flow may involve different mineral phases deforming via distinct mechanisms, one phase undergoing fracturing while another flows viscously. In the presence of water, fracture propagation may occur at stress intensity factors below the nominal fracture toughness of the rock due to stress corrosion, a mechanism where chemical reactions at crack tips weaken atomic bonds over time (Molaei & Kemeny, 2021). This enables fractures to grow and materials to fail under constant, subcritical stresses, a process known as brittle creep. Brittle creep depends strongly on the abundance and size of preexisting microfractures, making it particularly significant in fine-grained or microcracked rocks. Consequently, under a broad range of crustal conditions, especially near the BDT, brittle creep may represent the fastest active deformation mechanism (Brantut et al., 2013).

Ductile deformation, in contrast, is governed by temperature-activated processes such as atomic diffusion and dislocation movement. It is generally volume-conserving and exhibits a strong dependence on temperature and strain rate, but relatively little sensitivity to confining pressure under typical crustal conditions. Under low-stress conditions, diffusion creep, where strain rate varies linearly with stress, often dominates. Another mechanism is dissolution–precipitation creep, which is mediated by a fluid phase along grain boundaries and involves three steps: (1) dissolution of minerals at high-stress sites, (2) mass transport through the fluid, and (3) reprecipitation at lower-stress sites (Reber & Pec, 2018).

At the wellbore scale, brittle deformation typically manifests as breakouts and tensile failures, while semi-brittle deformation may involve a combination of shear and tensile failure accompanied by time-dependent creep. Under ductile conditions, deformation is dominated by creep with little to no fracturing (Figure 1).

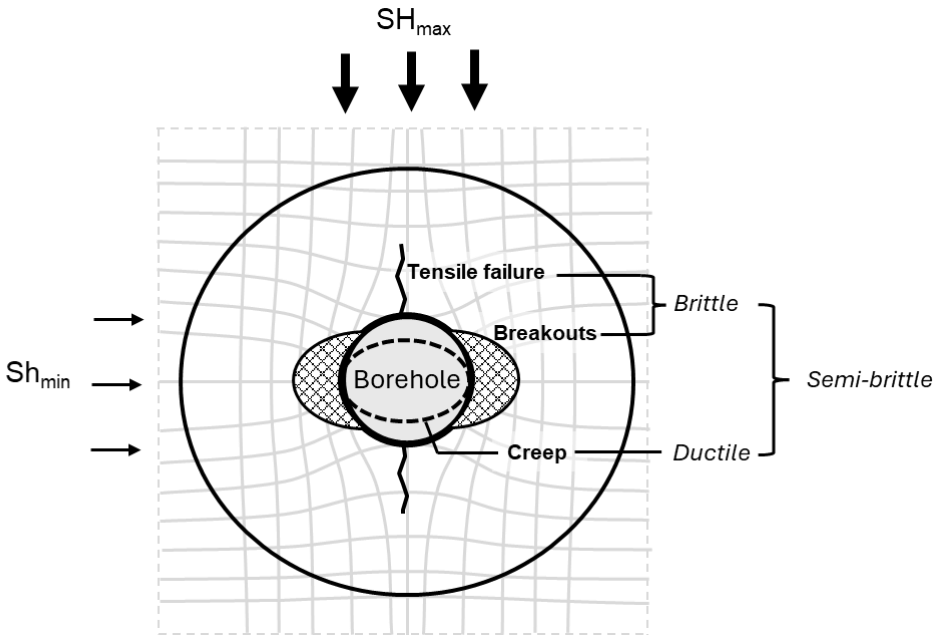


Figure 1. Conceptual illustration of deformation mechanisms around a borehole. Brittle behavior is expressed through tensile failure and breakouts, whereas semi-brittle deformation combines fracturing with time-dependent creep. Under fully ductile conditions, deformation occurs primarily by creep with no fracturing.

2.1 Deformation Mechanisms of Granite: Evolution and Controlling Factors

This section focuses on the evolution and sensitivity of the deformation mechanisms of granite under high-pressure, high-temperature conditions. Granite was selected as the reference material for basement rocks because it represents a major constituent of the continental crust. A compilation of experimental data from various sources was used to assess the mechanical response of granite at different stress and temperature regimes as presented in Figure 2a. At low confining stresses (<100 MPa) and temperatures below 200 °C, all granitic samples exhibit a brittle behavior with a low sensitivity to temperature changes, a conclusion consistent across multiple studies (Hoek & Martin, 2014; Violay et al., 2017; Wang et al., 2022; Meyer et al., 2024).

For confining stresses above 100 MPa, all data included in this review are specific to Westerly granite. Most of the experiments were conducted at target strain rates of approximately 1X10-5 s^{-1} (Griggs et al., 1960; Tullis & Yund, 1977; Wong, 1982; Violay et al., 2017). The reported confining stress in Figure 2a corresponds to effective confining stress, defined as the total confining stress minus the pore pressure.

The brittle behavior of granite shows two distinct trends: an initial slope up to approximately 150 MPa, and a second trend extending from 150 MPa to 500 MPa, see Figure 2a. Due to limited data in the transition zone between these slopes, the exact stress at which the transition occurs is difficult to determine. However, this two-slope behavior is well documented in classical studies and is beyond the scope of the current investigation (Byerlee, 1968; Kohlstedt et al., 1995). These brittle regimes were approximated using linear trend lines (black dashed lines). In addition to the brittle trends, Figure 2a includes two other curves: a blue dashed line, representing the confining stress at which the onset of semi-brittle behavior has been identified by various authors, and a solid line representing the Goetze criterion. The Goetze criterion is an empirical rule that defines the transition from frictional sliding to dislocation creep (Goetze, 1971; Kohlstedt et al., 1995).

Figure 2b illustrates the effect of increasing temperature and confining stress on rock strength. Strength decreases gradually up to approximately 400–500 °C and 400 MPa, as shown by the data enclosed within the dashed box. Beyond this range, the behavior becomes more variable, with occasional sharp drops in rock strength. These transitions are interpreted as marking the onset of the brittle-ductile transition, as discussed in more detail below.

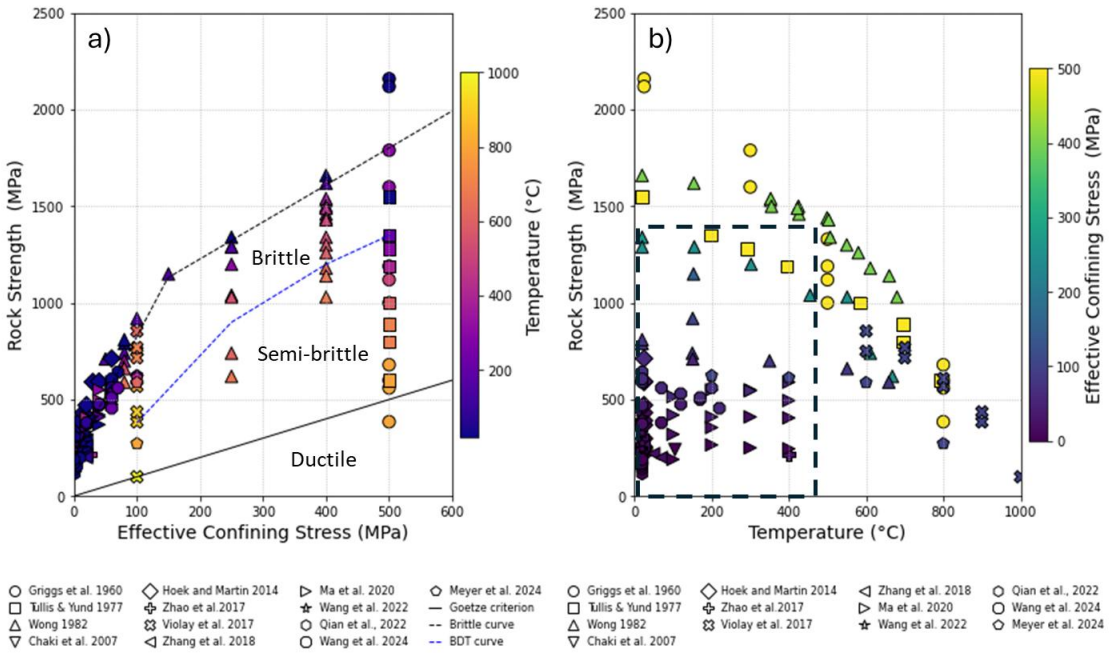


Figure 2. Stress-temperature conditions and deformation regimes of granite. (a) Rock strength as a function of confining stress, showing two distinct brittle regimes represented by black dashed linear trends. The blue dashed line indicates the approximate onset of semi-brittle behavior as identified by various authors. The solid line represents the Goetze criterion, marking the transition to ductile flow. (b) Rock strength as a function of temperature.

To better understand this transition, series of experiments conducted at fixed confining stresses (80, 100, 250, 400, and 500 MPa) and systematically increasing temperatures were reviewed to identify the thresholds at which

Westerly granite transitions from brittle to semi-brittle, and ultimately to fully ductile behavior. These experiments consistently show a progressive decrease in peak strength with increasing temperature (Figure 3).

At 80 and 100 MPa confining stress, results from Wong, (1982) and Violay et al., (2017) revealed a clear reduction in strength with increasing temperature. At 100 MPa, for example, peak stress declined from 815 MPa at 600 °C to 719 MPa at 900 °C, which was interpreted as evidence of increasing contributions from crystal-plastic deformation and stress corrosion cracking. Up to 800 °C, the failure mode remained brittle and dilatant; at 900 °C, deformation still involved shear fracturing but also exhibited net compaction, attributed to enhanced plasticity. At 1000 °C, the rock underwent fully ductile deformation with no signs of strain localization (Violay et al., 2017).

Across the range of confining stresses (80-500 MPa), a consistent trend was observed, rock strength decreased with increasing temperature. Up to about 500 °C and 400 MPa confining stress, the strength reduction was moderate (generally less than 20%). Beyond this threshold, however, a more accelerated decline in strength occurred. Post-failure observations showed well-developed shear fractures, even at higher temperatures, though fracture zones became broader, indicating a shift toward more distributed deformation (Wong, 1982). As explained above, a combination of brittle failure from shear fractures and distributed deformation contributing to the overall strain is the preferred configuration for semi-brittle flow.

The temperature at which failure becomes more stable, marked by smoother and more predictable stress drops, varies with confining stress. These transition temperatures were reported as follows: below 700 °C at 80 MPa, 550-600 °C at 250 MPa, 450-500 °C at 400 MPa, and ~300 °C at 500 MPa, as illustrated by the circles in Figure 3. It is important to note that these tests were performed under dry or gas-saturated conditions; the presence of water would significantly enhance stress corrosion and lower the transition temperature.

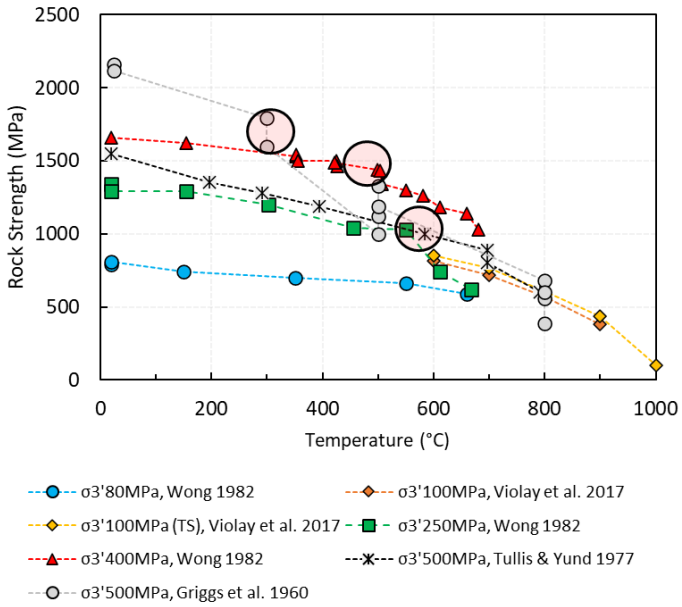


Figure 3. Transition stress and temperatures for semi-brittle behavior. Rock strength as a function of temperature at multiple confining stresses (80, 100, 250, 400, and 500 MPa). The curves illustrate the progressive decrease in strength with increasing temperature.

These results suggest that increasing confining stress stabilizes post-failure behavior and lowers the temperature at which the semi-brittle transition occurs (Wong, 1982). This interpretation is supported by the slope changes in the strength vs. temperature curves shown in Figure 3, which reflect a shift from a regime dominated by stress-dependent brittle failure to one less dependent on stress and more dependent on temperature. Thus, the effect of increasing confining stress is to shift the transition to a lower temperature.

At the microscale, the transition is driven by a combination of stress corrosion, dissolution–precipitation, and crystal-plastic creep, which together facilitate the progressive evolution from brittle to semi-brittle, and ultimately ductile deformation in Westerly granite under varying pressure–temperature conditions.

2.1.1 Effects of Water Saturation

The presence of water can significantly influence the creep deformation mechanisms in granitic rocks. Water plays a critical role in enabling time-dependent deformation, primarily through a process known as stress corrosion, where chemical reactions at crack tips facilitate subcritical crack growth (Reber & Pec, 2018). Stress corrosion occurs when water, acting as a chemically reactive agent, reduces the bond strength at the tips of microcracks. This process allows fractures to propagate even under stress intensity levels below the fracture toughness of the material. In silicate minerals, water weakens atomic bonds at the crack tip, enabling stable crack growth over extended periods at subcritical stress levels. As a result, water-saturated granite can undergo creep deformation more readily than its dry counterpart, since less mechanical energy is required to drive crack propagation (Lockner, 1993). According to Kohlstedt et al., (1995) even small amounts of fluid can significantly enhance creep and reduce fracture strength, including at relatively low temperatures. These observations highlight the importance of incorporating water phase behavior, pore pressure, temperature, and strain rate into constitutive equations, particularly for brittle sliding and semi-brittle flow regimes.

Based on this understanding, the strain rates of dry and wet Westerly granite were calculated using the power-law creep theory and the material parameters reported by Hansen & Carter (1983). Figure 4 shows the strain rate as a function of differential stress and temperature. As illustrated in Figure 4a and 4b, the wet granite reaches higher strain rates at lower stress and temperature levels compared to dry granite. In particular, the strain rate in wet granite increases much more rapidly at lower differential stresses, which can have significant implications in systems where the degree of rock saturation is unknown. While the difference between the two curves in Figure 4 may appear subtle due to the logarithmic scale, the underlying difference represents orders of magnitude.

As an example, consider a borehole wall subjected to a stress concentration of 400 MPa and a bottom-hole temperature of 500 °C, temperature conditions similar to those in the IDDP-2 project (Bromley et al., 2021). Under these conditions, the strain rate of wet Westerly granite is estimated to be 5.57X10-9 s^{-1}, compared to 1.94X10-10 s^{-1} for dry granite, more than an order of magnitude difference. If we consider a time length of one year and an initial wellbore diameter of 8.5 inches, the deformation in the dry granite scenario would be approximately 0.6% (1.32mm), while in wet granite it would reach 17.5% (37.5mm), a significant difference that could critically affect borehole integrity and operational viability.

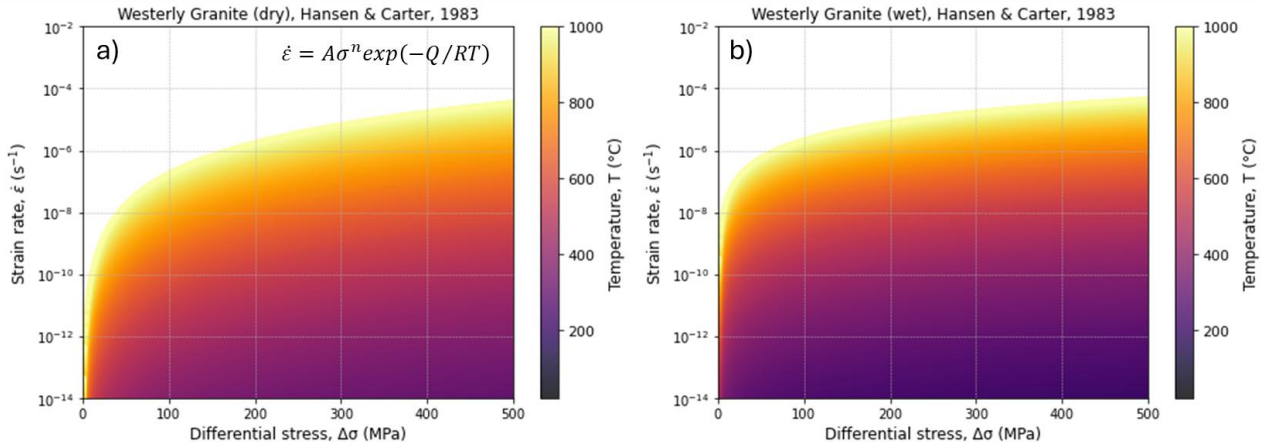


Figure 4. Strain rate for dry (a) and wet (b) Westerly granite as a function of differential stress and temperature, calculated using the power-law creep equation and parameters from Hansen & Carter (1983).

2.1.2 Influence of Confining Stress

It is widely recognized that as rocks transition from brittle to ductile deformation, the dependency of peak strength on confining stress decreases. This change is attributed to the suppression of dilatant cracking and the increasing contribution of volume-conserving time-dependent flow mechanisms (Byerlee, 1968; Wong, 1982). In the brittle regime, the compressive strength of intact, dry rocks is strongly influenced by confining stress and mineralogy, often in an approximately linear manner, and to a much lesser extent by temperature and strain rate. However, at higher confining stresses and temperatures, this linear relationship begins to break down as the stress dependence of strength diminishes (Kohlstedt et al., 1995).

In the ductile regime, rock strength becomes more sensitive to temperature and strain rate than to confining stress (Violay et al., 2017). Reber & Pec (2018) compiled an extensive dataset of deformation experiments on

quartz-rich rocks to characterize the brittle-ductile transition. They found that below 600 °C, the differential stress at failure exhibits a positive dependence on confining stress, with a typical ratio of approximately 2:1. However, at 650 °C, this dependency drops abruptly, indicating that rock strength becomes insensitive to confining stress and is instead controlled by time-dependent deformation mechanisms under laboratory conditions. In the semi-brittle regime, however, confining stress remains an important factor. Reber & Pec, (2018) noted that it strongly influences brittle creep by resisting the opening of wing cracks, modestly affects dislocation creep via water fugacity, and impacts dissolution-precipitation creep through changes in quartz solubility in aqueous fluids.

Effects on Rock Strength

As part of our ongoing analysis of compiled data for Westerly granite, Figure 5 illustrates the influence of confining stress on the strength of Westerly granite at different temperatures across the brittle-ductile transition. All experiments were conducted at strain rates of approximately 1x10-5 s^{-1}. Figure 5a shows the relationship between rock strength and confining stress at various temperatures, with trend lines representing least-squares fits through the data. These results demonstrate that the influence of confining stress on rock strength decreases as temperature increases. In agreement with the findings of Reber & Pec, (2018), Figure 5b shows the initial positive dependence of rock strength on confining stress at lower temperatures, following a roughly 2.5:1 ratio. However, this dependence drops sharply around 500 °C and becomes nearly negligible by 800 °C, consistent with a transition to viscous-dominated deformation.

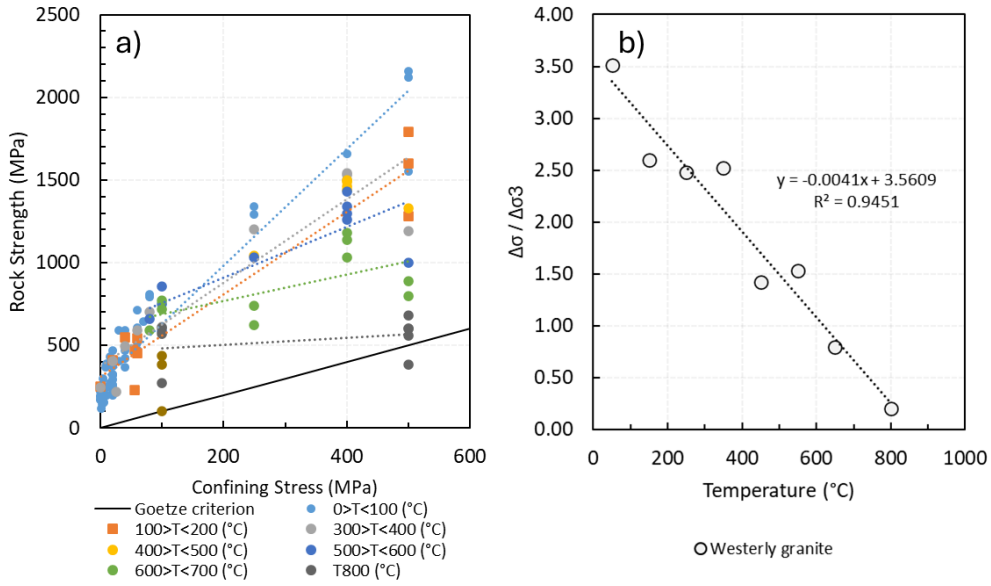


Figure 5. Influence of confining stress on the strength of Westerly granite across selected temperatures. (a) Rock strength vs. confining stress. (b) Slope of the differential stress-confining stress relationship as a function of temperature.

Effects on Strain Rate

To explore the potential dependency of confining stress on strain rate, the power-law flow formulation was applied using parameters compiled from Goetze, (1971); Carter et al., (1981); Rummel et al., (1986); Kirby & Kronenberg, (1987); Ranalli, (1997); and Violay et al., (2017) to estimate strain rates at temperatures relevant to geothermal applications (e.g., 400 °C). As shown in Figure 6, for dry Westerly granite, most curves indicate that as confining stress increases, the strain rate decreases significantly at a given differential stress. The confining stress (σ3) corresponds to the conditions at which the power-law creep parameters (A, n, and Q) were originally measured. Most curves exhibit a consistent trend, except for the curve corresponding to 100 MPa, which falls outside the range of the others. However, this observation should be interpreted with caution, as the dataset is limited. Consequently, additional experimental data are needed to verify whether the observed trend reflects a true confining stress dependency.

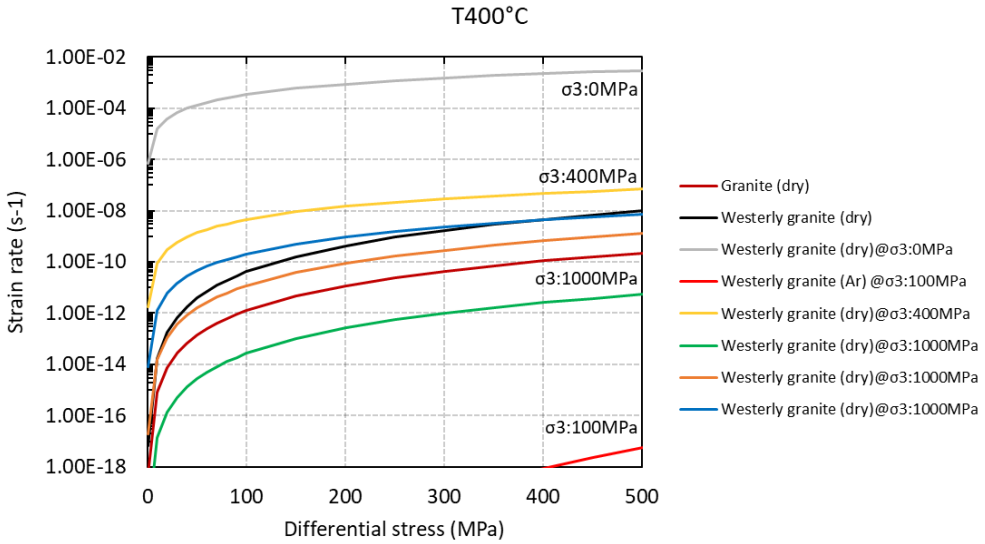


Figure 6. Calculated strain rate as a function of differential stress for dry Westerly granite at different confining stresses. Most curves show a decrease in strain rate with increasing confining stress, suggesting a potential confining stress dependency.

These findings are particularly relevant for geothermal applications, where deformation is likely governed by semi-brittle mechanisms. In such environments, differential stress, confining stress, temperature, and strain rate may strongly influence the overall mechanical behavior. At the wellbore scale, the confining stress is typically approximated by the lithostatic stress, while differential stresses arise from localized stress concentrations around the borehole. Additionally, the circulation of fluids causes continuous temperature fluctuations, which could induce significant short- and long-term changes in deformation response. Understanding these interactions is essential for ensuring short- and long-term borehole stability in ultra-deep geothermal settings.

3 EVIDENCE FROM ULTRA-DEEP DRILLING PROJECTS: WELLBORE CONVERGENCE

Observations from ultra-deep drilling programs provide clear evidence of time-dependent borehole deformation in crystalline basement rocks under high-pressure, high-temperature conditions. The most illustrative examples are the German Continental Deep Drilling Program (KTB) and the Siljan Ring borehole (Gravberg-1) in Sweden, both of which demonstrated borehole convergence and closure due to potential semi-brittle creep mechanisms.

In the KTB, which reached 9.1 km and a bottom-hole temperature of approximately 265 °C, severe wellbore instabilities developed below 7.5–8 km depth. These included breakouts, drilling-induced tensile fractures, and particularly undergauge zones associated with progressive borehole convergence. Caliper logs acquired three months after drilling (Figure 7) show deep sections where measured diameters (C2 = 177 mm) are smaller than the bit size (215.9 mm), confirming time-dependent closure of the borehole. This convergence was most pronounced in graphitic and chloritic paragneisses with strong foliation, where rock strength was anisotropic and reduced by the presence of weak mineral films and fluids. Despite increasing the mud weight to 1.4 kg/L, convergence continued and became a dominant operational challenge below 8 km. The most problematic interval, between 8.6 and 8.8 km, required continuous reaming for several months due to persistent narrowing of the borehole immediately after each trip (Borm et al., 1997; Emmermann & Lauterjung, 1997).

Microstructural analyses of cores from the deepest sections revealed healed microcracks, quartz dislocation structures, and solution–precipitation textures, all indicative of semi-brittle deformation. The combination of high differential in situ stress (~140 MPa), low permeability, and elevated temperature promoted slow viscoplastic flow consistent with the onset of the brittle–ductile transition (Dresen et al., 1997). Borehole convergence occurred preferentially in the direction of the maximum horizontal stress, suggesting stress-controlled time-dependent deformation rather than purely mechanical collapse.

These findings highlight that time-dependent borehole closure at KTB was far more detrimental to drilling progress than either breakouts or tensile failures. The deformation evolved over time, reflecting a creep-like response of the crystalline rock mass once temperature, stress, and pore-fluid effects combined to activate

diffusive and crystal-plastic mechanisms. Such behavior confirms that, even below 300 °C, crystalline rocks can undergo measurable time-dependent convergence when sufficiently stressed and fluid-assisted.

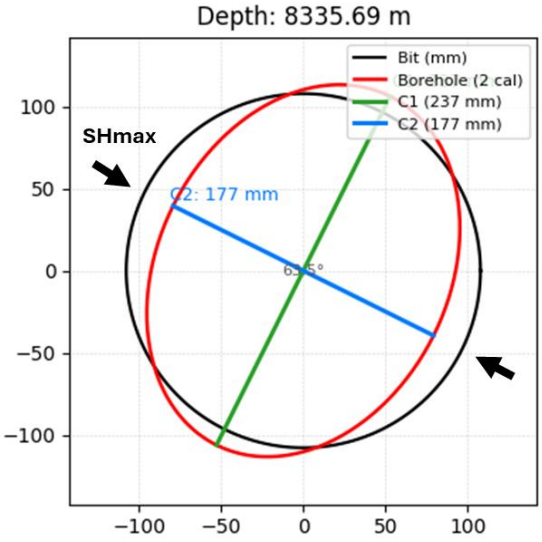


Figure 7. Caliper log from the KTB main borehole at a depth of 8335.69 m showing borehole convergence. One of the calipers (C2 = 177 mm) is smaller than the original bit size (215.9 mm), indicating time-dependent closure resulting from creep.

Comparable deformation behavior was observed in the Gravberg-1 borehole (Siljan Deep Drilling Project) in central Sweden, which penetrated 6.7 km into Precambrian granitic basement affected by dolerite intrusions and multiple fracture zones formed by a Devonian meteorite impact (Stephansson et al., 1989). In the Gravberg-1 well, where temperatures at target depth were estimated at ~100 °C, breakouts began at ~1.5 km and persisted to 4.8 km, while severe instability and “tight zones” appeared between 6.0 and 7.0 km, where the rock mass squeezed the borehole, reducing its diameter and causing frequent stuck-pipe events (Stephansson et al., 1989). These convergence zones, recorded by four-arm caliper logs, developed even under weighted mud (1.3-1.5 g/cm3) and produced operational difficulties closely resembling those at KTB. The nearby Stenberg-1 borehole reached 6.5 km and provided complementary stress data derived from Borehole Geometry Tool (BGT) calipers (Lund & Zoback, 1999). No image logs were available, and the authors reported borehole enlargements in all directions at several depth intervals, producing data gaps, but no evidence of viscoplastic convergence or creep-controlled closure. Instead, Stenberg-1 primarily records stress-induced breakouts and circumferential enlargements, consistent with a strike-slip to normal-faulting stress regime and a regional SH orientation of ~N53W.

The Kola Superdeep Borehole (SG-3) reached 12.2 km and ~220 °C in crystalline basement rocks. Although no under-gauge convergence was reported, increasing instability below 7 km reflected strong differential stresses and a transition toward quasi-plastic behavior at 10–12 km, marked by rising resistivity and reduced fluid content. According to Zhamaletdinov, 2020, this “impenetrability boundary” corresponds to the brittle–ductile transition, where rock strength and viscosity increase sharply. The Iceland Deep Drilling Project (IDDP-2), reaching 4.5 km and ~426 °C, experienced severe thermal and hydraulic instabilities from cooling-induced fracturing and loss of circulation within the sheeted-dike complex. Image logs confirmed breakouts and drilling-induced fractures, consistent with a brittle frictional regime, with the BDT estimated near 5.5–6 km depth (Friðleifsson et al., 2017; Peter-Borie et al., 2018).

Together, the KTB, Siljan, Kola, and IDDP-2 projects demonstrate that borehole deformation in crystalline basement rocks results from a complex combination of thermal, mechanical, and hydraulic processes. While convergence becomes more pronounced as temperatures approach ~250–300 °C, there is no single controlling factor that fully explains the onset of time-dependent closure. In several cases, particularly at lower-temperature sites such as the Gravberg-1, conditions including high differential stress, fluid saturation, microcrack connectivity, and mineral anisotropy likely promoted brittle creep, enabling measurable time-dependent deformation even below the classical brittle–ductile transition. Collectively, these observations indicate that both brittle and viscous mechanisms can contribute to borehole convergence, with their relative importance governed by the local stress state, temperature, and pore-fluid conditions. Understanding this

coupled behavior is critical for defining the operational limits and long-term stability of ultra-deep geothermal and scientific drilling projects.

4 CONCLUSIONS

This study reviewed deformation mechanisms operating across the brittle–ductile transition and examined their implications for wellbore stability in ultra-deep drilling. Experimental data on granite and field evidence from deep boreholes demonstrate that deformation in crystalline rocks is governed by an interaction of temperature, stress, water saturation, and microcrack structure. The onset of semi-brittle flow and creep-like convergence is not restricted to the crustal BDT but can also develop locally around the wellbore under high stress and fluid pressure, forming a local creep behavior that promotes time-dependent closure even at moderate temperatures (<300 °C). Borehole convergence observed in the KTB and Gravberg-1 exemplifies this phenomenon. These findings emphasize that both brittle creep and time-dependent flow contribute to wellbore deformation and that their relative importance depends on the local thermo-hydro-mechanical environment. Understanding this interaction is essential for predicting and managing stability in future ultra-deep geothermal and scientific drilling operations.

Acknowledgements

The authors gratefully acknowledge Eavor Technologies Inc. for supporting the preparation and presentation of this paper. The authors also thank Matej Pec and Emad Jahangir for their valuable insights and feedback.

REFERENCES

Borm, G., Engeser, B., Hoffers, B., Kutter, H. K., & Lempp, C. (1997). Borehole instabilities in the KTB main borehole. Journal of Geophysical Research: Solid Earth, 102(B8), 18507–18517. https://doi.org/10.1029/96JB03669

Brantut, N., Heap, M. J., Meredith, P. G., & Baud, P. (2013). Time-dependent cracking and brittle creep in crustal rocks: A review. Journal of Structural Geology, 52, 17–43. https://doi.org/10.1016/j.jsg.2013.03.007

Bromley, C., Axelsson, G., Asanuma, H., Manzella, A., & Dobson, P. (2021, October). Supercritical Fluids—Learning About the Deep Roots of Geothermal Systems from IEA Geothermal Collaboration. Proceedings World Geothermal Congress 2020+1.

Byerlee, J. D. (1968). Brittle-ductile transition in rocks. Journal of Geophysical Research, 73(14), 4741–4750. https://doi.org/10.1029/JB073i014p04741

Carter, N. L., Anderson, D. A., Hansen, F. D., & Kranz, R. L. (1981). Creep and Creep Rupture of Granitic Rocks. In N. L. Carter, M. Friedman, J. M. Logan, & D. W. Stearns (Eds.), Geophysical Monograph Series (pp. 61–82). American Geophysical Union. https://doi.org/10.1029/GM024p0061

Dresen, G., Duyster, J., Stöckhert, B., Wirth, R., & Zulauf, G. (1997). Quartz dislocation microstructure between 7000 m and 9100 m depth from the Continental Deep Drilling Program KTB. Journal of Geophysical Research: Solid Earth, 102(B8), 18443–18452. https://doi.org/10.1029/96JB03394

Emmermann, R., & Lauterjung, J. (1997). The German Continental Deep Drilling Program KTB: Overview and major results. Journal of Geophysical Research: Solid Earth, 102(B8), 18179–18201. https://doi.org/10.1029/96JB03945

Friðleifsson, G. Ó., Elders, W. A., Zierenberg, R. A., Stefánsson, A., Fowler, A. P. G., Weisenberger, T. B., Harðarson, B. S., & Mesfin, K. G. (2017). The Iceland Deep Drilling Project 4.5 km deep well, IDDP-2, in the seawater-recharged Reykjanes geothermal field in SW Iceland has successfully reached its supercritical target. Scientific Drilling, 23, 1–12. https://doi.org/10.5194/sd-23-1-2017

Goetze, C. (1971). High temperature rhelogy of westerly granite. Journal of Geophysical Research, 76(5), 1223–1230. https://doi.org/10.1029/JB076i005p01223

Griggs, D. T., Turner, F. J., & Heard, H. C. (1960). Chapter 4: Deformation of Rocks at 500° to 800° C. In Geological Society of America Memoirs (Vol. 79, pp. 39–104). Geological Society of America. https://doi.org/10.1130/MEM79-p39

Hoek, E., & Martin, C. D. (2014). Fracture initiation and propagation in intact rock – A review. Journal of Rock Mechanics and Geotechnical Engineering, 6(4), 287–300. https://doi.org/10.1016/j.jrmge.2014.06.001

Kirby, S. H., & Kronenberg, A. K. (1987). Rheology of the lithosphere: Selected topics. Reviews of Geophysics, 25(6), 1219–1244. https://doi.org/10.1029/RG025i006p01219

Kohlstedt, D. L., Evans, B., & Mackwell, S. J. (1995). Strength of the lithosphere: Constraints imposed by laboratory experiments. Journal of Geophysical Research: Solid Earth, 100(B9), 17587–17602. https://doi.org/10.1029/95JB01460

Lockner, D. (1993). Room temperature creep in saturated granite. Journal of Geophysical Research: Solid Earth, 98(B1), 475–487. https://doi.org/10.1029/92JB01828

Lund, B., & Zoback, M. D. (1999). Orientation and magnitude of in situ stress to 6.5 km depth in the Baltic Shield. International Journal of Rock Mechanics and Mining Sciences, 36(2), 169–190. https://doi.org/10.1016/S0148-9062(98)00183-1

Meyer, G. G., Shahin, G., Cordonnier, B., & Violay, M. (2024). Permeability partitioning through the brittle-to-ductile transition and its implications for supercritical geothermal reservoirs. Nature Communications, 15(1), 7753. https://doi.org/10.1038/s41467-024-52092-0

Molaei, F., & Kemeny, J. (2021, June 20). Investigation of Stress Corrosion Cracking in rocks, a reactive molecular dynamic simulation. 55th US Rock Mechanics/Geomechanics Symposium Held in Houston, Texas, USA, 20-23 June 2021. American Rock Mechanics Association, Houston, Texas, USA.

Peter-Borie, M., Loschetter, A., Merciu, I. A., Kampfer, G., & Sigurdsson, O. (2018). Borehole damaging under thermo-mechanical loading in the RN-15/IDDP-2 deep well: Towards validation of numerical modeling using logging images. Geothermal Energy, 6(1), 17. https://doi.org/10.1186/s40517-018-0102-7

Ranalli, G. (1997). Rheology of the lithosphere in space and time. Geological Society, London, Special Publications, 121(1), 19–37. https://doi.org/10.1144/GSL.SP.1997.121.01.02

Reber, J. E., & Pec, M. (2018). Comparison of brittle- and viscous creep in quartzites: Implications for semi-brittle flow of rocks. Journal of Structural Geology, 113, 90–99. https://doi.org/10.1016/j.jsg.2018.05.022

Rummel, F., Möhring-Erdmann, G., & Baumgärtner, J. (1986). Stress constraints and hydrofracturing stress data for the continental crust. Pure and Applied Geophysics, 124(4–5), 875–895. https://doi.org/10.1007/BF00879616

Stephansson, T. Savilahti, & B. Bjarnason (Eds.). (1989). Rock mechanics of the deep borehole at Gravberg, Sweden. In Paper presented at the ISRM International Symposium, Pau, France, August 1989.

Tullis, J., & Yund, R. A. (1977). Experimental deformation of dry westerly granite. Journal of Geophysical Research, 82(36), 5705–5718. https://doi.org/10.1029/JB082i036p05705

Violay, M., Heap, M. J., Acosta, M., & Madonna, C. (2017). Porosity evolution at the brittle-ductile transition in the continental crust: Implications for deep hydro-geothermal circulation. Scientific Reports, 7(1), 7705. https://doi.org/10.1038/s41598-017-08108-5

Wang, Z. H., Guo, L., Li, S. M., & Konietzky, H. (2022). Experimental Study on Physical and Mechanical Properties of Beishan Granite after Cyclic Heating and Cooling with Water. Lithosphere, 2021(Special 7), 5470799. https://doi.org/10.2113/2022/5470799

Wong, T.-F. (1982). Effects of temperature and pressure on failure and post-failure behavior of Westerly granite. Mechanics of Materials, 1(1), 3–17. https://doi.org/10.1016/0167-6636(82)90020-5

Zhamaletdinov, A. A. (2020). Fiftieth Anniversary of the Kola SG-3 Superdeep Borehole. Izvestiya, Atmospheric and Oceanic Physics, 56(11), 1401–1422. https://doi.org/10.1134/S0001433820110110